Laser performance of Yb^{3+}:YAG ceramic microchip lasers

Jun Dong*[a], Akira Shirakawa[a], Ken-ichi Ueda[a], Hideki Yagi[b], Takagimi Yanagitani[b], and Alexander A. Kaminskii[c]

[a]Institute for Laser Science, University of Electro-Communications, 1-5-1 Chofugaoka, Chofu, Tokyo 182 – 8585, Japan;

[b]Takuma Works, Konoshima Chemical Co., Ltd., 80 Kouda, Takuma, Mitoyo-gun, Kagawa 769-1103, Japan;

[c]Institute of Crystallography, Russian Academy of Sciences, Crystal Laser Physics Laboratory, Leninsky Pr. 59, Moscow 119333, Russia

ABSTRACT

The optical properties of Yb:YAG ceramic doped with different Yb concentrations are presented. The absorption coefficient at peak absorption wavelength of 940 nm increases linearly with Yb concentration in Yb:YAG ceramics. Low-threshold and highly-efficient continuous-wave (cw) laser-diode end-pumped Yb:YAG microchip ceramic laser with near-diffraction-limited beam quality was demonstrated at room temperature. Slope efficiencies of 79%, 67% and optical-to-optical efficiency of 60%, 53% at 1030 nm and 1049 nm, respectively were achieved for 1-mm-thick Yb:YAG ceramic plate (C_{Yb} = 9.8 at.%) under cw laser-diode pumping. Dual-wavelength operation at 1030 nm and 1049 nm with 5% transmission of the output coupler was achieved by varying pump power intensity. 1049 nm laser operation was automatically obtained by using 5% transmission output coupler when absorbed pump power is higher than 1 W. The lasers operate in multi-longitudinal-mode; the effect of pump power on the laser emission spectra for both wavelengths is addressed. The laser wavelength around 1030 nm shifts to short wavelength at low pump power region and then to red with increase of the absorbed pump power, while the laser wavelength around 1049 nm does not change with the pump power. Excellent laser performance indicates Yb:YAG ceramic laser materials could be potentially used in high-power solid-state lasers operating at 1030 nm, 1049 nm, or both wavelengths simultaneously. Laser-diode pumped low-threshold and highly-efficient passively Q-switched Yb:YAG ceramic microchip laser with Cr^{4+}:YAG ceramic as saturable absorber has also been demonstrated. The slope efficiency is as high as 37%, and the optical-to-optical efficiency is as high as 29% for 89% initial transmission of Cr^{4+}:YAG ceramic. The pulse width of 380 ps and peak power of over 82 kW at repetition rate of 12.4 kHz was obtained. Single-longitudinal-mode oscillation and wide-separated multi-longitudinal-mode oscillation due to etalon effect of Cr^{4+}:YAG thin plate was achieved depending on the pump power level.

Keywords: Yb:YAG, ceramic lasers, microchip laser, dual-wavelength operation, laser-diode pumping, multi-longitudinal-mode oscillation, Q-switched

1. INTRODUCTION

Ceramic laser materials [1-3] fabricated by the vacuum sintering technique and nanocrystalline technology [4] have gained more attentions as potential solid-state laser materials in recent years because they have several remarkable advantages compared with single crystal laser materials, such as high concentration and easy fabrication of large-size ceramics samples, multilayer and multifunctional ceramics laser materials [5], low cost and mass production. Efficient and high power laser operation in Nd^{3+} doped yttrium aluminum garnet ($Y_3Al_5O_{12}$ or YAG) and Yb^{3+} doped Y_2O_3 ceramic lasers has been demonstrated [1, 6]. The investigation of Yb^{3+} doped materials has gained a lot of attention because ytterbium lasers have several advantages over Nd^{3+} doped materials, such as absence of the cross relaxation, excited-state absorption, low thermal loading, broad absorption band, long fluorescence lifetime, high quantum efficiency, and so on. YAG is an attractive laser host material because of its excellent thermal, chemical and mechanical properties. Yb:YAG has been a promising candidate for high-power laser-diode (LD) pumped solid-state lasers [7, 8]. However, there are defects such as cores, light-scattering particles and concentration gradient along the growth axis in Yb:YAG crystals grown from the melt by Czochralski (CZ) and other methods. Nanocrystalline ceramic technology will be a more promising method to obtain large-size, high-optical-quality Yb:YAG ceramic laser material. The fabrication

Solid State Lasers XVI: Technology and Devices, edited by Hanna J. Hoffman, Ramesh K. Shori, Norman Hodgson,
Proc. of SPIE Vol. 6451, 645118, (2007) · 0277-786X/07/$15 · doi: 10.1117/12.699056

and laser operation of Yb:YAG ceramics doped with 1 at.% Yb^{3+} ions have been reported [9], but the efficiency of such Yb:YAG ceramic laser is low owing to the low ytterbium concentration. The quasi-four-level laser system of Yb:YAG requires high pumping intensity to achieve highly efficient laser operation. Thin Yb:YAG gain medium with high doping activator concentration will be more favorable for thermal management. Recently efficient Yb:YAG ceramic laser has been reported [10]. Passively Q-switched Yb:YAG laser with Cr^{4+}:YAG as saturable absorber was first demonstrated by using Ti:sapphire laser as pump source [11]. Passively Q-switched Yb:YAG microchip laser with 530 ps pulse width has been obtained by using SESAM [12]. Recently, laser-diode pumped Cr,Yb:YAG microchip laser with pulse width of 440 ps, peak power over 53 kW has been demonstrated [13], however, owing to co-doping of chromium ions with Yb into YAG host, the fluorescence lifetime decreases and there is absorption of pump power by Cr^{4+}, the efficiency of such compact microchip laser is low (18.5% slope efficiency and 10% optical-to-optical efficiency). Sandwiched configuration of gain medium and saturable absorber should be an alternative way to achieve highly efficient laser operation with short pulse width. Short resonator cavity length will permit short pulse operation, separation of gain medium and saturable absorber will eliminate the defects introducing in Cr,Yb:YAG, Cr^{4+}:YAG only act as a saturable absorber, not an additional loss to pump power. The performance of passively Q-switched Yb:YAG ceramic laser with Cr^{4+}:YAG ceramic as saturable absorber has been reported recently [14]. In this paper, we report on the spectral properties of high ytterbium doped YAG ceramic and highly efficient laser performance of LD-pumped microchip ceramic lasers at 1030 nm and 1049 nm, and passively Q-switched all ceramic Yb:YAG/Cr:YAG microchip laser. The slope efficiency is as high as 79% and the optical-to-optical efficiency is over 60%, even when the laser is working at room temperature without active cooling system, just using conduction cooling through the copper sample holder. The results show that $Y_3Al_5O_{12}$ ceramics doped with 9.8 at.% Yb^{3+} ions have excellent optical quality. The laser characteristics (output power and laser spectrum) under different output couplings are investigated as a function of the pump power. We also investigate the performance of all ceramics Yb:YAG/Cr:YAG microchip laser, the laser pulses with pulse energy of 31.3 μJ, pulse width of 380 ps at repetition rate of 12.4 kHz were obtained when the absorbed pump power was 1.3 W, the corresponding peak power of over 82 kW was obtained in this all-ceramics passively Q-switched Yb:YAG laser with Cr:YAG ceramic as saturable absorber. The pulse characteristics of this all-ceramics passively Q-switched Yb:YAG/Cr:YAG microchip laser were investigated in details as a function of the pump power. Also the laser radiation spectra were addressed as a function of the absorbed pump power.

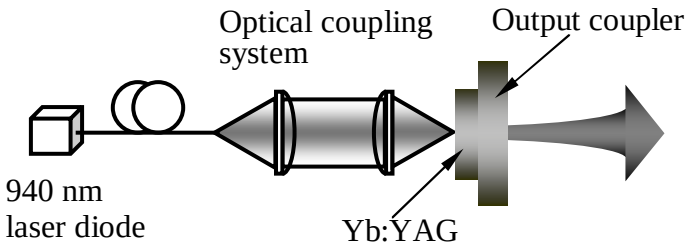

Fig. 1 Schematic diagram of laser-diode pumped microchip Yb:YAG ceramic laser.

2. EXPERIMENTS

The absorption spectra of Yb:YAG ceramics doped with 9.8, 12 and 20 at.% Yb^{3+} ions concentrations are measured by using ANDO white light source and emission spectrum of these Yb:YAG ceramics are also measured by using 940 nm laser-diode as pump source and the emission signal was detected with an optical spectrum analyzer at room temperature. The laser experiment was carried out with a plane-parallel, 1-mm-thick Yb:YAG ceramic plate (C_{Yb} = 9.8 at.%) as gain medium. The schematic diagram of experimental setup is shown in Fig. 1. One surface of the Yb:YAG ceramic plate is anti-reflection-coated at 940 nm and highly reflecting at 1030 nm to act as a cavity mirror of the laser. The other surface of the Yb:YAG is anti-reflection-coated at 1030 nm to reduce the cavity loss. Four plane-parallel mirrors were used as output couplers with different transmissions of 5%, 10%, 15% and 20% at 1.03 μm. The overall cavity length was about 1 mm. A 35-W fiber-coupled 940 nm LD with a core diameter of 100 μm and numerical aperture of 0.22 was used as the pump source. Two lenses of 8 mm focal length were used to focus the pump beam on the ceramic rear surface and to

produce a pump light footprint in the ceramics of about 100 μm in diameter. About 95% of the total pumping power is incident on the Yb:YAG ceramic plate after the coupling optics. The Yb:YAG laser was operated at room temperature without active cooling of the active element.

3. RESULTS AND DISCUSSIONS

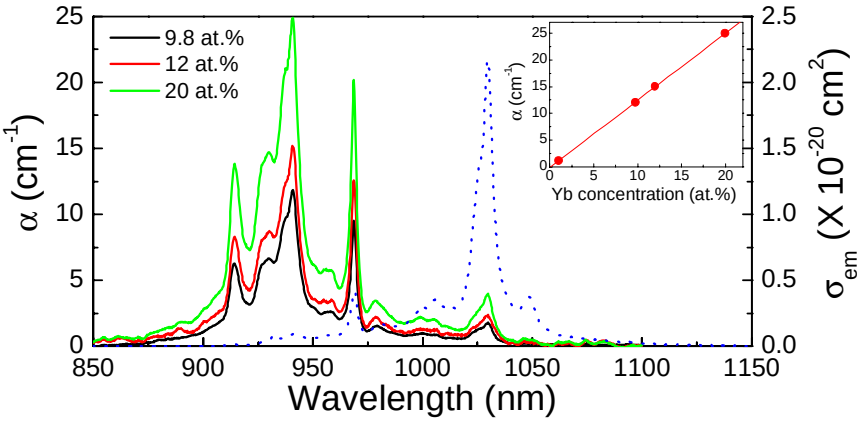

Fig. 2 Absorption coefficient (solid lines) and effective emission cross section (dotted line) of YAG ceramics doped with different Yb^{3+} ion concentrations at room temperature. The inset shows the variation of the absorption coefficient as a function of ytterbium doping concentration for Yb:YAG ceramics.

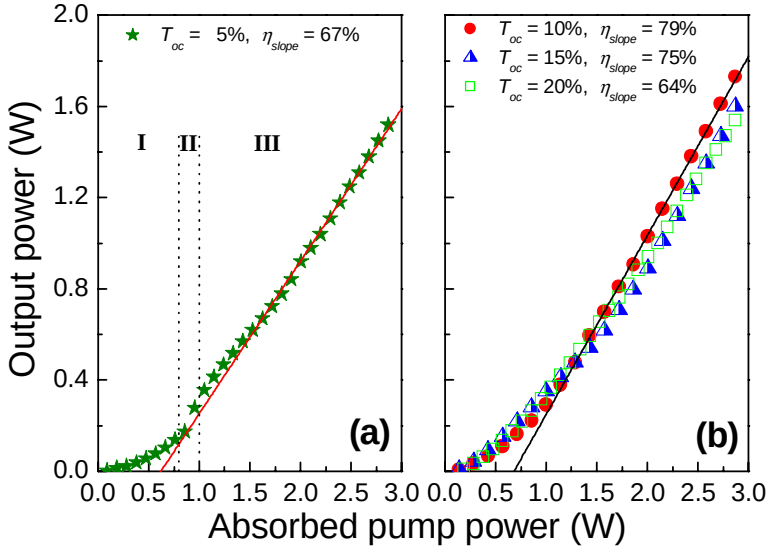

Fig. 3 Output power as a function of the absorbed pump power for different transmissions of the output coupler. (a) Transition from 1030 nm to 1049 nm oscillation with increase of pump power for T_{oc} = 5%, I, 1030 nm oscillation, II, dual-wavelength oscillation at 1030 nm and 1049 nm, III, 1049 nm oscillation; (b) 1030 nm oscillation for T_{oc} = 10%, 15% and 20%, respectively. The solid lines are the linear fitting for T_{oc} = 5% and 10%, respectively.

Fig. 2 shows the room temperature absorption and emission spectra of Yb:YAG ceramics contain 9.8, 12 and 20 at.% of ytterbium activators. The absorption and emission spectra of Yb:YAG ceramics are identical to those of Yb:YAG single crystals [15]. The peak absorption coefficient at 940 nm increases linearly with Yb activator concentration, as shown in inset of Fig. 1. Two main emission peaks are centered at 1030 nm and 1049 nm, the effective peak emission cross section (2.2×10^{-20} cm^2) at 1030 nm is about 6 times of that at 1049 nm.

The laser output power of microchip Yb:YAG ceramic lasers as a function of the absorbed pump power for different output couplers is shown in Fig. 3. The absorbed pump power threshold increases from 82 mW to 240 mW when the transmission of the output coupler (T_{oc}) increases from 5% to 20%. The output power increases linearly with the absorbed pump power when the pump power is well above the pump power threshold, which is the nature of quasi-four-level system, the high efficiency can be achieved by using high pump power intensity. The maximum output power was achieved with T_{oc} = 10%. Output power of 1.73 W was measured when the absorbed pump power was 2.87 W, and the slope efficiency was about 79%, the optical-to-optical efficiency is as high as 60% for T_{oc} = 10%. To our best knowledge, the slope efficiency of 79% and optical-to-optical efficiency of 60% are the highest slope efficiency and optical-to-optical efficiency achieved even in LD-pumped Yb:YAG ceramic microchip laser at room temperature just cooling the Yb:YAG sample by air. The measured slope efficiencies are 67%, 75% and 64% for T_{oc} = 5%, 15% and 20%, respectively. For T_{oc} = 5%, the laser operates at 1030 nm when the absorbed pump power is above pump power threshold and kept lower than 0.8 W; the laser oscillates at 1030 nm and 1049 nm simultaneously when the absorbed pump power is from 0.8 W to 1 W. The intensity of laser at 1030 nm decreases and intensity of laser at 1049 nm increases with absorbed pump power. The ceramic laser oscillates at 1049 nm when the absorbed pump power is higher than 1 W. The cause of the change of laser wavelength and dual-wavelength operation for Yb:YAG ceramic laser with T_{oc} = 5% is attributed to the quasi-four level nature of Yb:YAG material and the local temperature rise due to the heat generated at high pump power. The local temperature rise inside Yb:YAG gain medium has a great effect on the thermal population distribution of terminated laser level for 1030 nm, therefore the reabsorption around the strong emission peak of 1030 nm will increase, the threshold for 1030 nm oscillation will increase, however, the local temperature rise has little effect on the reabsorption loss around the weak emission peak of 1049 nm for Yb:YAG ceramics, there is a tradeoff between 1030 nm and 1049 nm oscillations. With further increase of the local temperature, the laser prefers to oscillate at 1049 nm than at 1030 nm with T_{oc} = 5%. The lasers oscillate at 1030 nm when the transmission of the output coupler is 10% or higher. The round-trip cavity loss, L, was estimated to be less than 5% from the measured values of the pump power threshold for different transmission of the output couplers according to the formula [16], $-\ln R = 2KP_{thr} - L$, where R is the reflectivity of the output coupler, P_{thr} is the pump power threshold and K is the pumping coefficient defined as the product of all the coefficients that lead to the population of the upper laser state.

The laser output beam profile was monitored using a charge coupled device camera both in the near field and the far field of the output coupler. The output laser transverse intensity profile was close to fundamental transverse electromagnetic mode in all the pump power range. The near-diffraction-limited beam quality M^2 of less than 1.1 for microchip Yb:YAG ceramic lasers was achieved.

The microchip Yb:YAG ceramic laser spectrum was analyzed by using an ANDO AQ6317 optical spectrum analyzer. The laser spectra of these lasers indicate several longitudinal modes oscillate simultaneously (around 1049 nm for T_{oc} = 5% when absorbed pump power is higher than 0.8 W and around 1030 nm when T_{oc} is 10%, 15% and 20%, respectively). For T_{oc} = 5%, four longitudinal modes oscillate at 1030 nm when the pump power is just over threshold, while six longitudinal modes oscillate with further increase of the pump power when absorbed pump power is kept lower than 0.8 W, as shown in Fig. 4(a). Dual-wavelength oscillation of Yb:YAG ceramic laser was observed when the absorbed pump power was kept between 0.8 W and 1 W, the intensity and number of longitudinal modes at 1030 nm decrease and number of longitudinal modes around 1049 nm increases with increase of the pump intensity. The laser spectra show that Yb:YAG ceramic laser oscillates around 1049 nm when the absorbed pump power is above 1 W. The longitudinal modes around 1049 nm increase with absorbed pump power (as shown in Fig. 4(a)). The separation of two close longitudinal modes is measured to be 0.3 nm. The longitudinal mode structures are different from those with equal spacing around 1030 nm (see Fig. 4(b)). The wide separation between longitudinal modes clearly shows that there is strong mode hoping and mode-competition between longitudinal modes around 1049 nm. This may be caused by flatter emission spectra around 1049 nm than around 1030 nm for Yb:YAG ceramics (as shown in Fig. 1) and the gain distribution along the Fabry-Perot resonator. For T_{oc} = 10%, the number of oscillating longitudinal modes was found to increase from three, just above threshold, to seven at higher pump power, as shown in Fig. 4(b). The separation of each longitudinal mode under different pump power was about 0.29 nm. The separation of the longitudinal modes in a laser cavity was given by

[16] $\Delta\lambda = \frac{\lambda^2}{2L_c}$, where L_c is the optical length of the resonator. For 1-mm-thick Yb:YAG planar-parallel gain medium studied here, Δλ was calculated to be 0.2915 nm, 0.302 nm with the laser wavelength of 1030 nm and 1049 nm, respectively, which were in good agreement with the experimental data. The linewidth at each mode was measured to be less than 5.7 GHz, i.e. the resolution limit of the instrument. The laser wavelengths around 1049 nm laser emission spectra nearly does not change with the absorbed pump power for T_{oc} = 5%, however, for T_{oc} is 10% or higher, the laser emission spectrum (around 1030 nm) shifts to the shorter wavelength when absorbed pump power is lower than 1 W and then shifts to the longer wavelength with the absorbed pump power when the absorbed pump power is higher than 1 W. The short wavlength shift of the laser lines around 1030 nm is caused by the strong gain at short wavelength of Yb:YAG ceramics, the effect of local temperature rise on the red shift of emission spectrum of Yb:YAG ceramics is not enough to compete the gain at short wavelength at low pump power. The red shift of the laser lines around 1030 nm at high pump power (> 1 W) is caused by the emission spectrum of Yb:YAG shifts to longer wavelength with increase of the temperature [15, 17] due to more heat generated inside the gain medium with the pump power. For 1049 nm oscillation, although the emission spectrum of Yb:YAG gain medium at 1049 nm shifts to longer wavelength with temperature, the emission spectrum around 1049 nm is flatter than that around 1030 nm. The effect of the temperature on the gain at 1049 nm is smaller than that at 1030 nm, therefore, the laser wavelengths around 1049 nm are nearly independent on the pump power.

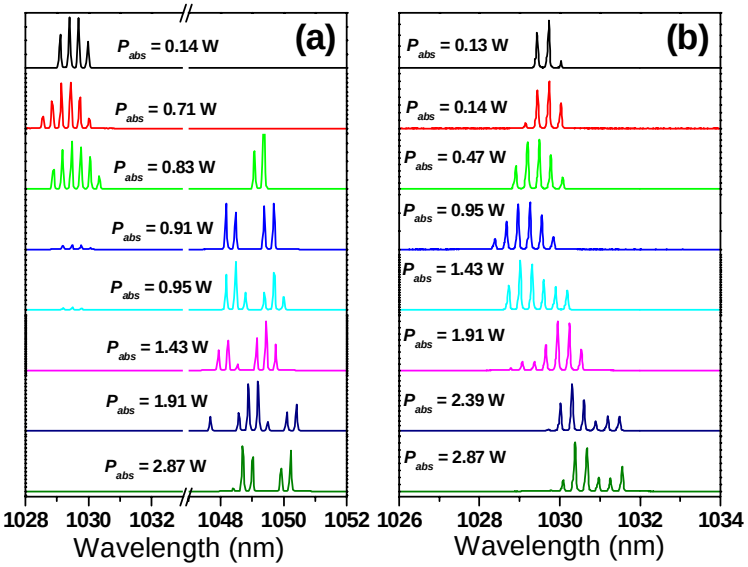

Fig. 4 Laser spectra of Yb:YAG ceramic lasers under different pump power levels for (a) T_{oc} = 5% and (b) T_{oc} = 10%.

4. PASSIVELY Q-SWITCHED ALL CERAMIC YB:YAG/CR:YAG MICROCHIP LASER

Fig. 5 shows the absorption spectrum of Cr:YAG ceramic doped with 0.5 at% Cr at room temperature, the absorption and emission spectra of Yb:YAG ceramics contain 9.8 at.% of ytterbium activators are also included in this figure for comparison. The absorption spectrum of Cr^{4+}:YAG ceramic is identical to those from Cr^{4+}:YAG single crystal previously reported [18, 19]. The absorption band centered at 612 nm (from 570 nm to 750 nm) belongs to the $^3B_1(^3A_2) \rightarrow {}^3A_2,{}^3E(^3T_1)$ transitions of Cr^{3+}. The absorption band centered at 1030 nm (from 750 nm to 1200 nm) is due mainly to the $^3B_1(^3A_2) \rightarrow {}^3A_2(^3T_1)$ transition and merely to the $^3B_1(^3A_2) \rightarrow {}^3E(^3T_2)$ transition of Cr^{4+}. The absorption coefficients of Cr^{4+}:YAG at 940 nm and 1030 nm are 4.2 $cm^{-1}$and 6 cm^{-1}, respectively. The main absorption peak of Yb:YAG is centered at 940 nm, the main emission peak is centered at 1030 nm. There is a strong absorption at 940 nm of Cr^{4+}:YAG, about 70% of that at 1030 nm, therefore, Cr^{4+} ions in YAG acts not only as saturable absorber at laser wavelength at 1030 nm, but also absorb the pump power, the waste of the pump power by Cr^{4+} ions in Cr,Yb:YAG can not be

neglected. The best way is to separate Yb:YAG and Cr:YAG, thus, composite Yb:YAG/Cr^{4+}:YAG ceramic will be better than co-doped Cr,Yb:YAG self-Q-switched laser crystal or ceramic.

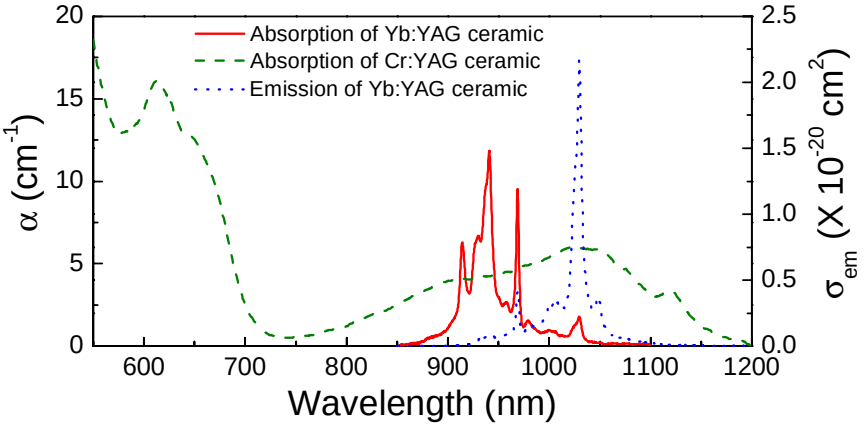

Fig. 5 The absorption spectrum of Cr^{4+}:YAG ceramic doped with 0.5 at.% Cr at room temperature and the absorption and emission spectra of Yb:YAG ceramic doped with 9.8 at.% Yb.

Fig. 6 shows a schematic diagram of experimental setup for passively Q-switched Yb:YAG ceramic microchip laser with Cr^{4+}:YAG ceramic as saturable absorber. A plane-parallel, 1-mm-thick Yb:YAG ceramic doped with 9.8 at.% Yb as gain medium. One surface of the ceramic was coated for anti-reflection at 940 nm and total reflection at 1.03 μm acting as one cavity mirror. The other surface was coated for high transmission at 1.03 μm. A 0.2-mm-thick Cr^{4+}:YAG ceramic with 89% initial transmission, acting as Q-switches, was sandwiched between Yb:YAG sample and a plane-parallel output coupler with 20% transmission. Total cavity length was 1.2 mm. A high-power fiber-coupled 940 nm laser diode with a core diameter of 100 μm and numerical aperture of 0.22 was used as the pump source. Two lenses of 8-mm focal length were used to focus the pump beam on the crystal rear surface and to produce a pump light footprint in the crystal of about 100 μm in diameter. The laser was operated at room temperature. The Q-switched pulse profiles were recorded by using a fiber-coupled InGaAs photodiode with a bandwidth of 16 GHz, and a 7 GHz Tektronix TDS7704B digital phosphor oscilloscope. The laser spectrum was analyzed by using an optical spectrum analyzer. The laser output beam profile was monitored using a CCD camera both in the near-field and the far-field of the output coupler.

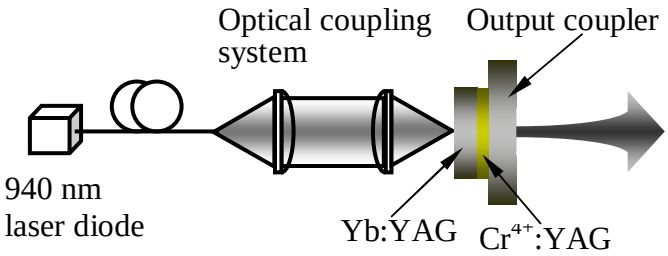

Fig. 6 A schematic diagram of laser-diode pumped passively Q-switched Yb:YAG ceramic microchip laser using Cr^{4+}:YAG ceramic as saturable absorber.

Average output power as a function of absorbed pump power and some laser spectra were shown in Fig. 7. The absorbed pump power threshold is about 0.25 W. Single-longitudinal-mode oscillation at 1030.4 nm was obtained when the absorbed pump power was kept below 0.6 W. Above this value, the laser exhibited two-mode oscillation and three-mode oscillation as shown in the inset of Fig. 7. Average output power increases linearly with absorbed pump power, the slope efficiency is about 37%. Maximum average output power of 390 mW was obtained when the absorbed pump power was 1.33 W, corresponding to optical-to-optical efficiency of 29%. There is coating damage occurrence with further increase

of the pump power. The coating damage was caused by the high intracavity intensity and low damage threshold of the coating, which can be avoided by improving the coating quality or increase of the transmission of the output coupler to reduce the intracavity laser intensity. Single-longitudinal-mode oscillation at 1030.4 nm was obtained when the absorbed pump power was kept below 0.6 W. Above this value, the laser exhibited two-mode oscillation when the absorbed pump power was kept below 0.9 W. A third-mode appeared besides the first-mode when the absorbed pump power was higher than 0.9 W. The separation between first-mode and second-mode was measured to be 1.24 nm, which is five times wider than the separation between the longitudinal modes (0.24 nm) in the laser cavity filled with gain medium predicted by [16] $\Delta\lambda_c = \lambda^2/2L_c$, where L_c is the optical length of the resonator, λ is laser wavelength. The separation between first-mode and third-mode was measured to be 0.24 nm, which is the same value determined by the laser cavity. The cause of wide separation between first-mode and second-mode is attributed to Cr^{4+}:YAG thin plate which acts as an intracavity titled etalon to select longitudinal modes [16]. For 0.2-mm-thick Cr^{4+}:YAG thin plate, because the ratio of cavity length to the thickness of Cr^{4+}:YAG thin plate is an integer, the resonant modes coinciding with the peak transmission of Cr^{4+}:YAG thin plate will oscillate and other resonant modes will be suppressed to oscillate, therefore, the separation between the output laser modes is determined the free spectral range of Cr^{4+}:YAG etalon to be 1.24 nm. The appearance of the third-mode besides first mode was caused by the high laser intensity of the cavity mode besides the highest gain and Cr^{4+}:YAG thin plate can not suppress the oscillation of this mode at high pump power. Of course, the possible oscillating laser modes are governed by the gain profile and non-linear mode coupling effect between the possible output modes. The linewidth of each mode was less than 0.02 nm, limited by the resolution of optical spectra analyzer. The central wavelength of 1030.4 nm shifts to longer wavelength, which is caused by the temperature dependent emission spectrum of Yb:YAG crystal [15]. The relative intensity of each mode changes with pump power, resulting the fluctuation of the output pulse trains, which is caused by the cross-saturation mechanism due to the strong spatial hole burning effect in Yb:YAG to couple the longitudinal modes via population gratings and nonlinear absorption of Cr^{4+}:YAG saturable absorber [20]. The output laser transverse intensity profile was close to TEM_{00} and was near-diffraction-limited with M^2 of less than 1.05. It should be noted that stable single-longitudinal-mode oscillation could be obtained by increasing pump beam diameter incident on the laser ceramic at higher pump power.

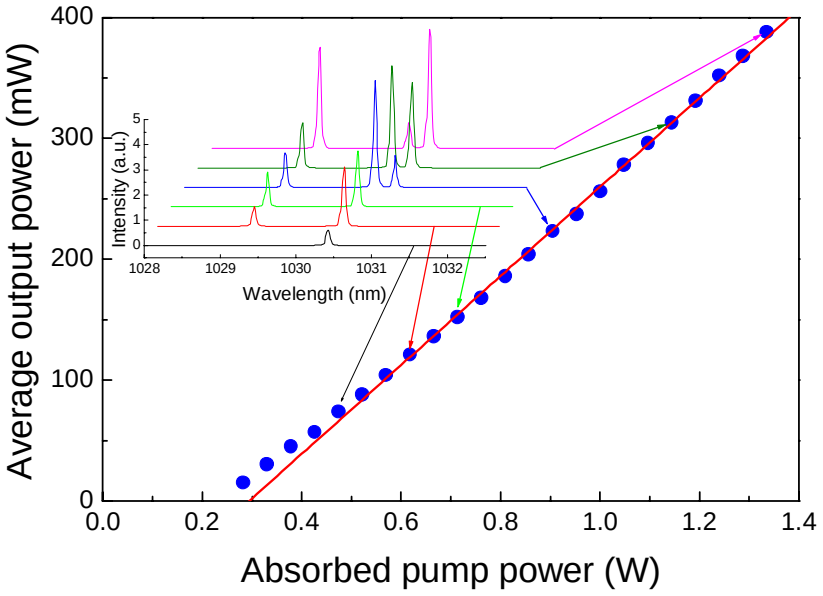

Fig. 7 Average output power as a function of the absorbed pump power for passively Q-switched Yb:YAG/Cr^{4+}:YAG ceramic microchip laser. Inset shows the laser spectra under different pump power.

Fig. 8 shows the output pulse with pulse duration of 380 ps and pulse energy of 31.3 μJ. Because the absorption cross section of Cr^{4+}:YAG is much larger than the emission cross section of Yb:YAG ceramic, the result pulse width can be estimated as follows [11],

$$t_p = \frac{0.86 t_r}{\gamma_{sat.r}} \left[\frac{\delta(1+\delta)\eta}{\delta - \ln(1+\delta)} \right] \tag{1}$$

where t_r is cavity round-trip time, η is the energy extraction efficiency of the laser pulse given by the implicit relationship $\eta(1+\delta) = -\ln(1-\eta)$, and $\delta = \gamma_{sat,r} / (\gamma_{par,r} + \gamma_{op})$ is the ratio of saturable loss, $\gamma_{sat,r}$, to unsaturable cavity loss, $\gamma_{par,r}$ is the round-trip unsaturable intracavity parasitic loss, γ_{op} is the output coupling loss. By taking these experimental data γ_{op} = 0.223, $\gamma_{par,r}$ = 0.105, $\gamma_{sat,r}$ = 0.25 for T_0 = 89%, into Eq. (1), the pulse widths of this kind of passively Q-switched Yb:YAG ceramic microchip lasers were estimated to be 248 ps for T_0 = 89%, which is in fair agreement with the experimental pulse width. The discrepancy between measured pulse width and expected pulse width is attributed to the thermal effects within the active medium and some uncertainties in the determination of unsaturable parasitic intracavity loss and saturable loss.

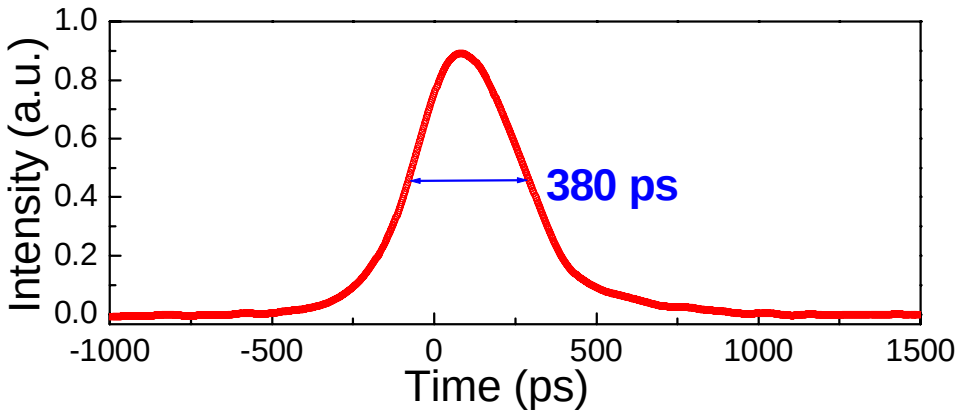

Fig. 8 Passively Q-switched laser pulse with 380 ps pulse width (FWHM) and 31.3 μJ pulse energy, corresponding to peak power of over 82 kW.

Fig. 9 shows pulse energy, pulse repletion rate, pulse width and peak power as a function of the absorbed pump power. Pulse energy increases from 16.5 μJ to 31.3 μJ with the absorbed pump power and pulse energy tends to saturation when the absorbed pump power is greater than 0.4 W. Repetition rate increases linearly from 910 Hz to 12.4 kHz with absorbed pump power. The error bars indicate the increase of in timing jitter at high repetition rate, and the timing jitter is less than 5% even at high pump power. Pulse width (FWHM) decreases from 460 ps to 380 ps very slowly with the absorbed pump power. Pulse width decreases faster at low pump power than at high pump power, and pulse width tends to be a constant at high pump power. Peak power of passively Q-switched Yb:YAG microchip laser increases from 36 kW to 82 kW with absorbed pump power. The shortest pulse width of 380 ps was obtained when the absorbed pump power of 1.33 W without coating damage, which is shorter than those obtained by using SESAM as saturable absorber for passively Q-switched Yb:YAG microchip laser [12] and Cr,Yb:YAG microchip laser [13]. Maximum peak power of over 82 kW was obtained when the absorbed pump power is 1.33 W. In addition, Q-switched laser pulses with pulse energy of 31 μJ and peak power over 82 kW at repetition rate of 12.4 kHz show this passively Q-switched Yb:YAG/ Cr^{4+}:YAG ceramic microchip laser more potential compact source to generate laser pulses with high pulse energy and high peak power.

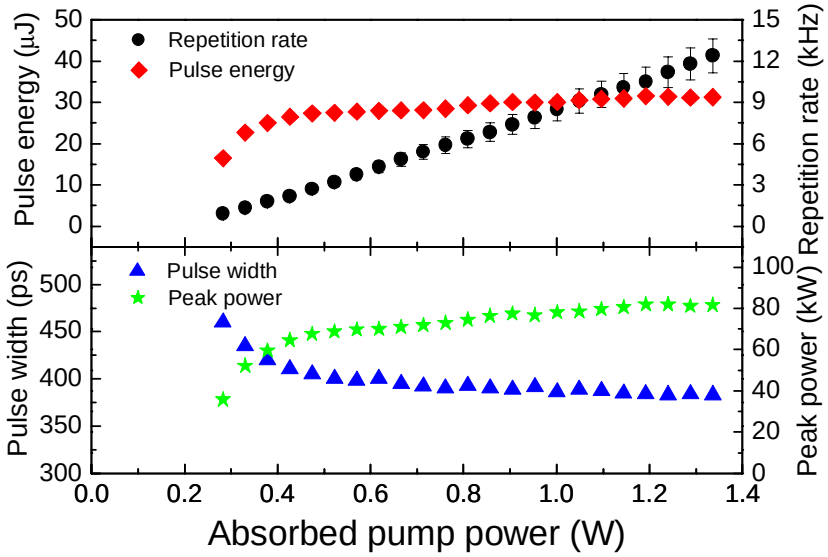

Fig. 9 Pulse energy, pulse repetition rate, pulse width (FWHM) and peak power of passively Q-switched all ceramic Yb:YAG/Cr^{4+}:YAG microchip laser as a function of the absorbed pump power.

5. CONCLUSIONS

In conclusion, efficient laser operation of LD end-pumped microchip Yb:YAG ceramics was demonstrated both at 1030 nm and 1049 nm. The laser was operated at room temperature just cooling by the air. The slope efficiency of as high as 79%, 67% and optical-to-optical efficiency of over 60% and 53% was achieved for 1030 nm and 1049 nm laser operations, respectively. The beam quality factor (M^2) at full pump power range was measured to be less than 1.1. The laser oscillation wavelength can be changed with 5% transmission of output coupler by varying pump power intensity incident on Yb:YAG ceramics. 1049 nm laser operation was automatically obtained by using 5% transmission output coupler when absorbed pump power is higher than 1 W. The laser wavelength around 1030 nm shifts to short wavelength at low pump power region and then to red with increase of the absorbed pump power, while the laser wavelength around 1049 nm does not change with the pump power. The laser experiments show that Yb:YAG ceramics doped with 9.8 at.% Yb have very good optical quality and can be a very good material for high-power laser operating at 1030 nm and 1049 nm. Also efficient passively Q-switched Yb:YAG ceramic microchip laser with Cr^{4+}:YAG ceramic as saturable absorber has been achieved, slope efficiency as high as 37% and optical-to-optical efficiency of 29% have been obtained by using 89% initial transmission of Cr^{4+}:YAG saturable absorber. Laser pulses with 380 ps pulse duration and 31.3 μJ pulse energy has been achieved, peak power of over 82 kW was obtained. Cr^{4+}:YAG thin plate also acts as an etalon to select longitudinal modes. Stable single-longitudinal-mode oscillation could be obtained at high pump power by increasing pump beam diameter. Laser performance of microchip Yb:YAG/Cr^{4+}:YAG ceramic lasers can be further improved by controlling concentrations in composite Yb:YAG/Cr^{4+}:YAG ceramic with the help of the vacuum sintering technique and nanocrystalline technology [4].

Acknowledgement **This work was supported by the 21st Century Center of Excellence (COE) program of Ministry of Education, Science, Sports and Culture of Japan. One of us (A. A. K.) wishes to acknowledge the Russian Foundation for Basic Research.**

REFERENCES

[1] J. Lu, K. Ueda, H. Yagi, T. Yanagitani, Y. Akiyama and A. A. Kaminskii, "Neodymium-doped yttrium aluminum garnet ($Y_3Al_5O_{12}$) nanocrystalline ceramics - a new generation of solid-state laser and optical materials," J. Alloys Comp. **341,** 220 - 225 (2002).

[2] J. Lu, K. Takaichi, T. Uematsu, A. Shirakawa, M. Musha, K. Ueda, H. Yagi, T. Yanagitani and A. A. Kaminskii, "Yb^{3+}:Y_2O_3 ceramics - a novel solid-state laser materials," Jpn. J. Appl. Phys. **41,** L1373 - L1375 (2002).

[3] J. Lu, K. Takaichi, T. Uematsu, A. Shirakawa, M. Musha, K. Ueda, H. Yagi, T. Yanagitani and A. A. Kaminskii, "Promising ceramic laser material: highly transparent Nd^{3+}:Lu_2O_3 ceramic," Appl. Phys. Lett. **81,** 4324 -4326 (2002).

[4] T. Yanagitani, H. Yagi and Y. Hiro, "Production of yttrium aluminium garnet fine powders for transparent YAG ceramic," Japan Patent No. 10-101411, (1998).

[5] H. Yagi, T. Yanagitani, K. Yoshida, N. M and K. Ueda, "Highly efficient flashlamp-pumped Cr^{3+} and Nd^{3+} codoped $Y_3Al_5O_{12}$ ceramic laser," Jpn. J. Appl. Phys. **45,** 133 - 135 (2006).

[6] J. Kong, D. Y. Tang, B. Zhao, J. Lu, K. Ueda, H. Yagi and T. Yanagitani, "9.2-W diode-end-pumped Yb:Y_2O_3 ceramic laser," Appl. Phys. Lett. **86,** 161116 (2005).

[7] A. Giesen, H. Hugel, A. Voss, K. Wittig, U. Brauch and H. Opower, "Scalable concept for diode-pumped high-power solid-state lasers," Appl. Phys. B **58,** 365 - 372 (1994).

[8] T. S. Rutherford, W. M. Tulloch, E. K. Gustafson and R. L. Byer, "Edge-pumped quasi-three-level slab lasers: design and power scaling," IEEE J. Quantum Electron. **36,** 205 - 219 (2000).

[9] T. Takaichi, H. Yagi, J. Lu, A. Shirakawa, K. Ueda, T. Yanagitani and A. A. Kaminskii, "Yb^{3+}-doped $Y_3Al_5O_{12}$ ceramics - A new solid-state laser material," Phys. Status Solidi (a) **200,** R5 - R7 (2003).

[10] J. Dong, A. Shirakawa, K. Ueda, H. Yagi, T. Yanagitani and A. A. Kaminskii, "Efficient Yb^{3+}:$Y_3Al_5O_{12}$ ceramic microchip lasers," Appl. Phys. Lett. **89,** 091114 (2006).

[11] J. Dong, P. Deng, Y. Liu, Y. Zhang, J. Xu, W. Chen and X. Xie, "Passively-Q-switched Yb:YAG laser with Cr^{4+}:YAG as a saturable absorber," Appl. Opt. **40,** 4303 - 4307 (2001).

[12] G. J. Spuhler, R. Paschotta, M. P. Kullberg, M. Graf, M. Moser, E. Mix, G. Huber, C. Harder and U. Keller, "A passively Q-switched Yb:YAG microchip laser," Appl. Phys. B **72,** 285 - 287 (2001).

[13] J. Dong, A. Shirakawa, S. Huang, Y. Feng, T. Takaichi, M. Musha, K. Ueda and A. A. Kaminskii, "Stable laser-diode pumped microchip sub-nanosecond Cr,Yb:YAG self-Q-switched laser," Laser Phys. Lett. **2,** 387 - 391 (2005).

[14] J. Dong, A. Shirakawa, K. Takaichi, K. Ueda, H. Yagi, T. Yanagitani and A. A. Kaminskii, "All ceramic passively Q-switched Yb:YAG/Cr^{4+}:YAG microchip laser," Electron. Lett. **42,** 1154 - 1156 (2006).

[15] J. Dong, M. Bass, Y. Mao, P. Deng and F. Gan, "Dependence of the Yb^{3+} emission cross section and lifetime on the temperature and concentration in ytterbium aluminum garnet," J. Opt. Soc. Am. B **20,** 1975 - 1979 (2003).

[16] W. Kochner, *Solid State Laser Engineering* (Springer-Verlag, Berlin Germany, 1999).

[17] G. A. Bogomolova, D. N. Vylegzhanin and A. A. Kaminskii, "Spectral and lasing investigations of garnets with Yb^{3+} ions," Sov. Phys. JETP **42,** 440 - 446 (1976).

[18] H. Eilers, U. Hommerich, S. M. Jacobsen, W. M. Yen, K. R. Hoffman and W. Jia, "Spectroscopy and dynamics of Cr^{4+}:$Y_3Al_5O_{12}$," Phys. Rev. B. **49,** 15505 - 15513 (1994).

[19] A. G. Okhrimchuk and A. V. Shestakov, "Absorption saturation mechanism for YAG:Cr^{4+} crystals," Phys. Rev. B **61,** 988 - 995 (2000).

[20] J. Dong and K. Ueda, "Longitudinal-mode competition induced instabilities of Cr^{4+},Nd^{3+}:$Y_3Al_5O_{12}$ self-Q-switched two-mode laser," Appl. Phys. Lett. **87,** 151102 (2005).

* Email: dong@ils.uec.ac.jp; Phone: +81-0424-43-4708; Fax: +81-0424-85-8960.